IOP Publishing Smart Materials and Structures
Smart Mater. Struct. **26** (2017) 035044 (11pp) https://doi.org/10.1088/1361-665X/aa5bd6

The strengthening effect of 1D carbon materials on magnetorheological plastomers: mechanical properties and conductivity

Jiaqi Xu[1], Shouhu Xuan[1,2,3], Haoming Pang[1] and Xinglong Gong[1,3]

[1] CAS Key Laboratory of Mechanical Behavior and Design of Materials, Department of Modern Mechanics, University of Science and Technology of China, Hefei 230027, People's Republic of China
[2] National Synchrotron Radiation Laboratory, University of Science and Technology of China, Hefei, 230027, People's Republic of China

E-mail: xuansh@ustc.edu.cn and gongxl@ustc.edu.cn

Received 19 December 2016, revised 20 January 2017
Accepted for publication 24 January 2017
Published 15 February 2017

Abstract

This work reported novel multifunctional carbon filler-doped magnetorheological plastomers (CMRPs) and their magnetic–mechanical–conductive coupling properties. Here, the one-dimensional carbon fillers, such as carbon micro-fibers (CFs), carbon nanotubes (CNTs) and their mixtures (CFs and CNTs) were dispersed into the matrix for the final product. It was found that the CMRPs with 7.5 wt% CFs and 0.5 wt% CNTs had an excellent magnetorheological (MR) effect (2200%) and magnetic field dependent electrical property. Specifically, the resistance was reduced by two orders of magnitude with the magnetic field increasing from 0 to 900 mT. Moreover, the relationship between resistance and strain was also discovered. The resistance increased by three orders of magnitude due to the amplitude of oscillation, which was 10% in the absence of the magnetic field, while the resistance would decrease by three orders of magnitude under a 900 mT magnetic field. The variation range of the resistance increased with the increasing oscillation amplitude, and the period of the resistance was half of the period of the strain. To conclude, the possible mechanism for the multifunctional properties was discussed.

Keywords: magnetorheological, carbon, oscillation shear, strain

(Some figures may appear in colour only in the online journal)

1. Introduction

Magnetorheological (MR) materials are a kind of magnetic intelligent material which are prepared by dispersing soft magnetic particles in different matrixes. Usually, the MR materials are mainly classified as magnetorheological elastomers (MREs), magnetorheological fluids (MRFs) and magnetorheological gels (MRGs). Because the MR materials have controllable rheological properties and their mechanical behavior can be changed rapidly and reversibly, the MR materials are widely applied in dampers [1–4], shock absorbers [5–7], and isolators [8–11] etc. Recently, magnetorheological plastomers (MRPs) which are composed of carbonyl iron powders in soft polymer matrixes have attracted increasing interest because of their high MR effects and stability. Upon applying an external magnetic field, the iron powders in MRPs arranged into particle chains. After removing the magnetic field, the chain-like structures can be maintained for a period of time and the storage modulus of MRPs was still high. However, the matrix of MRFs had no restriction on the iron powder particles, and the storage modulus of MRFs was almost zero after removing the magnetic field. The matrix of MREs was mostly rubber, so it had large elasticity. After removing the magnetic field, the

[3] Authors to whom any correspondence should be addressed.

Table 1. Compositions of CMRPs.

Sample No.	1	2	3	4	5	6	7	8	9	10
Polyurethane (g)	10	10	10	10	10	10	10	10	10	10
CF (wt%)	0	0	0	0	8	15	7.5	7	14.5	14
CNT(wt%)	0	4	6	8	0	0	0.5	1	0.5	1

iron powder particles moved due to the recovery of deformation, which broke the chain structure of particles. Owning to the unique magnetic field dependent microstructure and mechanics, the MRPs have a broad application prospects.

The mechanical properties of the MR materials are highly dependent on the matrix, additives, particles, and interfaces between the particles and matrix. In consideration of the special physical and chemical characteristics in the MRPs, the additives play critical roles in determining the MR behavior. It was reported that the inorganic additives were favorable for improving the mechanical properties of MR materials. For example, adding the silicon carbide into the matrix could enhance the mechanical properties and durability of the MREs [12]. The organoclay [13] and plate-like iron particles [14] could improve the dispersibility and stability of the iron particles in MRFs. However, few works have been done on studying the influence of additives on the MRPs.

Carbon materials are often used as composite fillers due to their excellent mechanical and electrical properties. 1D carbon nanotubes (CNTs) and carbon micro-fibers (CFs) were doped in the matrices of polymer [15], cement mortar [16], silicon carbide [17], metal [18], rubber [19] and others to form multifunctional composites, thus achieving high shear strength, bending strength, stiffness and durability [20, 21]. Moreover, because of the excellent conductivity of the CNTs, CNT composites are widely used in electrodes [22, 23], sensors [24, 25], super capacitors [26, 27]. Though the conductivity of the CF was not so good, the uniform distribution of the CFs in the polymer matrix also enables good mechanical properties. The combination of CFs and other conductive fillers, such as graphite [28], carbon black [29] and silver nanowires [30], in the matrix can both improve the conductivity and mechanical properties. More importantly, the CFs and CNTs hybrid additives also exhibit such a synergistic effect [15, 31, 32].

Multifunctional MR materials with magnetic–mechanical–conductive coupling properties are attractive in various areas of application, such as sensors, dampers, etc. Therefore, the 1D carbon fillers have been used to construct various MR materials with enhanced mechanical properties and conductivity. Li *et al* found that a small number of CNTs could improve the shear storage modulus of conventional MREs [33]. By wrapping the polymethyl methacrylate coated iron particles with multi-walled CNTs, the rheological properties in MRFs can be clearly enhanced [34]. Moreover, some researchers poured the MRFs into the CNT foams to improve their compression capacity by applying a magnetic field [35]. Recently, Jang *et al* developed a multifunctional MRE sensor composed of

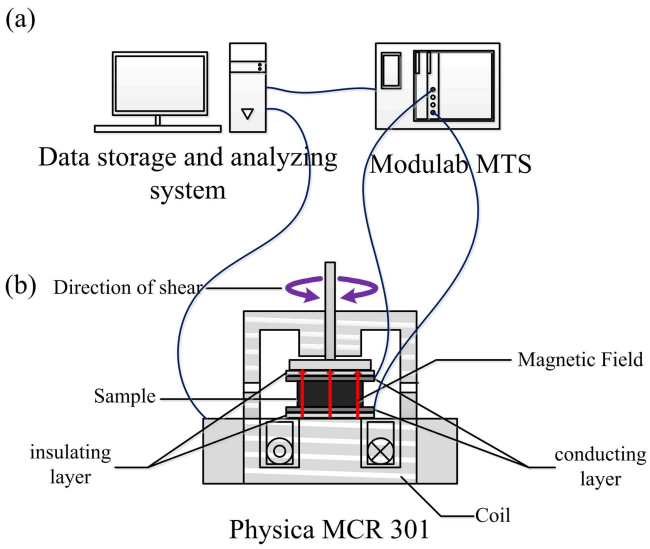

Figure 1. Schematic of the test device including: (a) a modulab material test systems, data storage and analyzing system; (b) a commercial rheometer equipped with a magneto-controllable accessory MRD180.

polydimethylsiloxane mixed with ferromagnetic particles and CNTs. It was found to be sensitive to the strain under the magnetic field [36]. The nickel-coated multi-walled CNTs were also dispersed in the MRGs to improve the storage modulus and damping properties [37]. Due to the importance of MRPs, the investigation of the carbon filler-doped MRPs was attractive for both academic study and practical applications. For example, the graphite doped conductive MRPs could be used to construct a magnetically dependent on–off switch [38]. Unfortunately, the systematic investigation of the effect of the 1D carbon fillers on the multifunctional MRPs has not been reported.

In this work, 1D carbon filler-doped magnetorheological plastomers (CMRPs) were prepared by dispersing both CFs and CNTs in MRPs via a solution mixing method. The mechanical properties and conductivity of CMRPs with different contents of CF and CNT were investigated. A optimum CFs/CNTs ratio was obtained for achieving the synergistic effect. The influences of strain and magnetic field on the resistance were studied and the structure-evolution mechanism was discussed. Finally, the relationships between the resistance and the oscillation frequency and amplitude in a shear oscillation mode were carefully analyzed. Because of their excellent electrical and mechanical properties, they present broad potential in sensors and dampers.

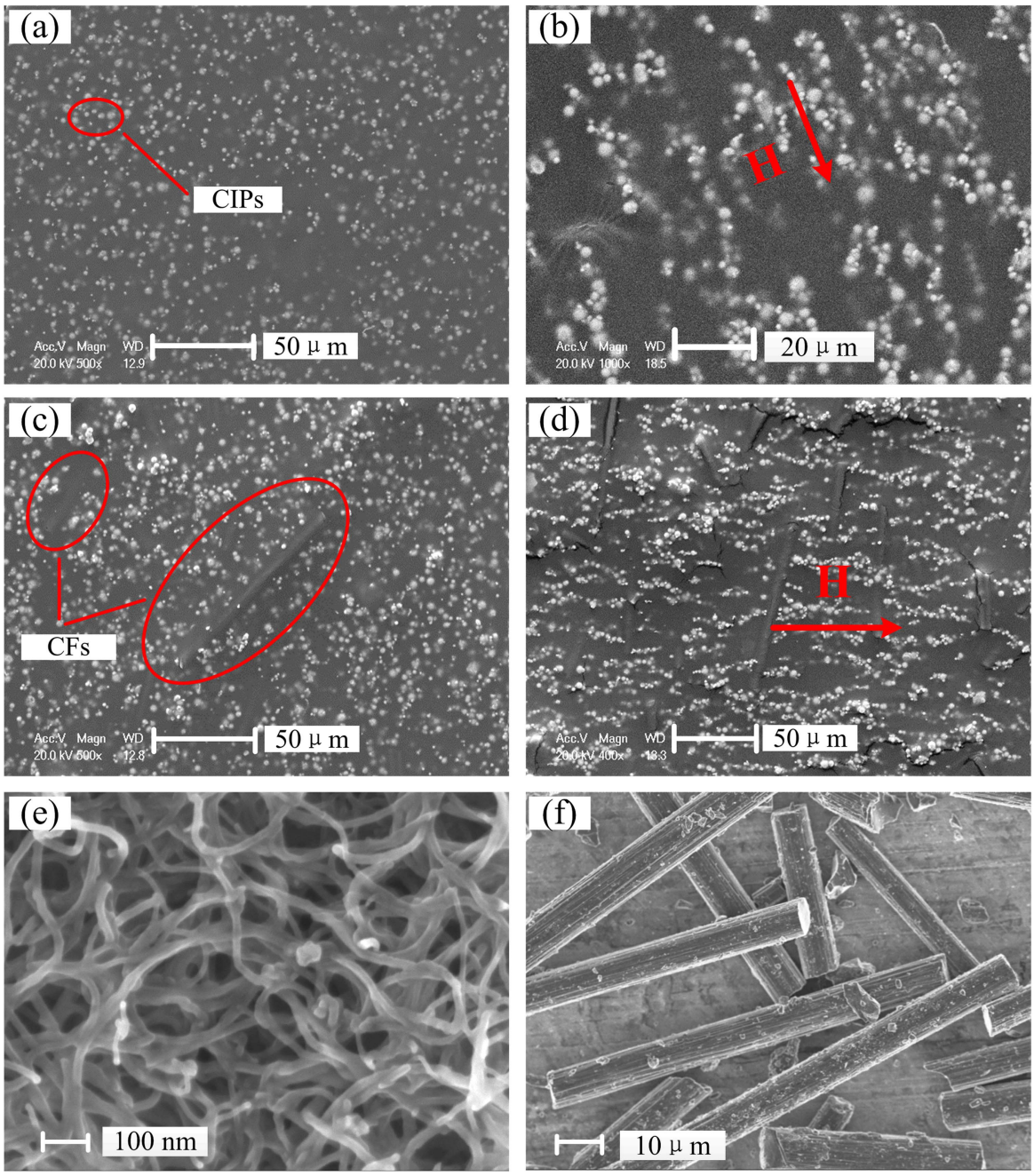

Figure 2. SEM images of (a) MRPs and (c) CMRPs without pre-configuration; (b) MRPs and (d) CMRPs after pre-configuration. The red arrow represents the direction of the magnetic field. (e) and (f) were the SEM images of CNTs and CFs.

2. Experimental

2.1. Raw materials

The raw materials are: polypropylene glycol (PPG-1000, Sinopec Group Co. Ltd, China), toluene diisocyanate (TDI, 2, 4-TDI at B80%, 2, 6-TDI at B20%, Tokyo Chemical Industry Co. Ltd, Japan), diethylene glycol (DEG, Sinopharm Chemical Reagent Co. Ltd, Shanghai, China), carbonyl iron powders (CIPs, type CN, BASF aktiengesellschaft, Germany), carbon nanotubes (CNTs, Conductive Materials of Luelida Co. Ltd, Xinxiang City, Henan province, China) (Conductivity: 100 S cm^{-1}), carbon fibers (CFs, New Material Technology of Zhongli Co., Ltd, Cangzhou City, Hebei province, China) (Conductivity: 700 S cm^{-1}), sodium dodecyl benzene sulfonate (SDBS, Sinopharm Chemical Reagent Co. Ltd, Shanghai, China), acetone and alcohol (Sinopharm Chemical Reagent Co. Ltd, Shanghai, China).

2.2. Sample preparation

Firstly, polyurethane was prepared as the polymer matrix for MRP. TDI and PPG with a molar ratio of 3:1 were added to a flask and continuously stirred for 2 h. The reaction temperature was maintained at 80 °C. Later, the temperature was set

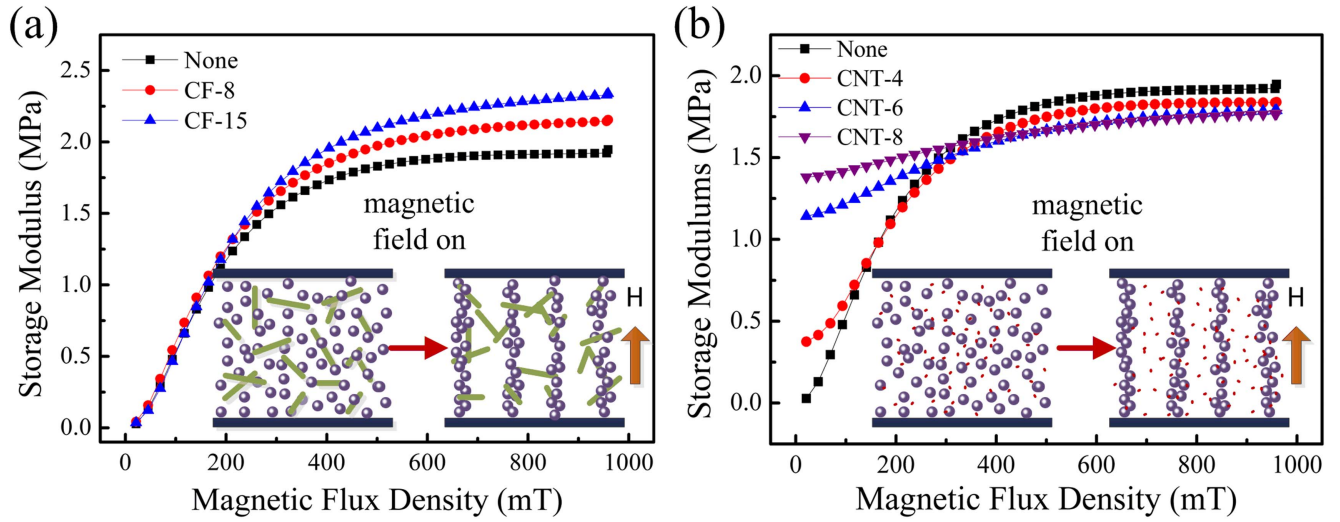

Figure 3. The storage modulus of CMRPs in different magnetic flux density: (a) CMRPs with different CF contents corresponding to 8 wt%, 15 wt%. (b) CMRPs with different CNT contents corresponding to 4 wt%, 6 wt%, 8 wt%. The microscopic evolution of the CMRPs after applying the magnetic field in (a) and (b). The purple balls represent the iron particles, the green lines represent the CFs, the red dots represent the CNTs.

to be 60 °C and DEG was added into the reactor. After half an hour, the preparation of the polyurethane was completed.

Then, CNTs and CFs were dispersed by a solution mixing method [39]. The carbon materials (CNTs and CFs) and SDBS with a weight ratio of 5:1 were homogeneously dispersed in 200 ml alcohol/acetone (1/1, v/v) mixed solvent in a flask by stirring for 2 h. A given amount of polyurethane was added into the solution and kept under ultrasonication for about 24 h. After that, the CIPs were added to the reactant under vigorous mixing. Finally, the product was moved to the drying oven to remove the residual ethanol and acetone.

By varying the CF and CNT concentrations, ten CMRPs were prepared. The compositions of CMRPs are shown in table 1.

2.3. Testing system

In our experiment, the mechanical and electrical properties of samples were carried out by a commercial rheometer (Physica MCR301, Anton Paar Co., Austria) equipped with a magneto-controllable accessory MRD180 (figure 1(b)), a modulab material test system (MTS, Solartron analytical, AMETEK advanced measurement technology, Inc., United Kingdom), and data storage and analyzing system (figure 1(a)). The sample was 1 mm in thickness, 20 mm in diameter, and the test voltage was 4 V. When testing the mechanical properties, the conductive layer and insulation layer in the rheometer were removed.

3. Results and discussion

After the preparation, the CIPs and CNTs/CFs were uniformly dispersed within the polyurethane matrix. Then, a magnetic field was applied, the CIPs (figure 2(a)) were assembled to form particle chains in the direction of the magnetic field (pre-configuration) (figure 2(b)). Due to the constraint of the matrix, the CIPs particle chains could be kept stable after removing the magnetic field. Figures 2(c) and (d) showed the SEM images of the CNTs/CFs doped MRP. Clearly, many large micro-rods with length around 100 μm were found in the matrix. Due to the large size scale, the micro-rods could not be driven along the magnetic field although the CIPs tended to be. The CFs were randomly dispersed within the matrix and formed a more complex three-dimensional structure together with the CIPs particle chains. Here, the size of the CNTs was rather smaller than the CFs (figures 2(e), (f)), thus the CNTs could hardly be observed in the SEM image due to the low concentration.

The mechanical properties of the CF doped CMRPs (CF-CMRPs) and CNT doped CMRPs (CNT-CMRPs) were tested by using a rheometer. Figure 3(a) showed the magnetic field dependent shear storage modulus (G') of CMRPs with different contents of CFs. Obviously, with increasing the magnetic flux density, G' increased. The G' of 8 wt% CF-CMRPs increased by 2.1 MPa with the magnetic flux density increasing from 0 to 900 mT. Here, the relative MR effect reached 5000%. (The MR effect was defined as $\Delta G'/G_0'$, in which $\Delta G'$ was an increase of storage modulus with the magnetic flux density increasing from 0 to 900 mT. G_0' was the storage modulus under a 0 mT magnetic field.). When the content of CF was 15%, the G' increased by 2.3 MPa and the relative MR effect reached as high as 6500%. Clearly, the CFs strengthened the MRPs and the MR performance increased with the CF content. Interestingly, the CNTs presented a inverse effect. As shown in figure 3(b), although the initial storage modulus (G_0') of CNT-CMRPs sharply increased with the CNT content, the saturation G' decreased, so that the MR effect was greatly reduced. Typically, the G_0' with 4 wt% CNT-CMRPs was 0.37 MPa, the saturation G' was 1.84 MPa, and the relative MR effect was 390% (figure 3(b)). As soon as the content of CNT reached 8 wt%, the G_0' increased to

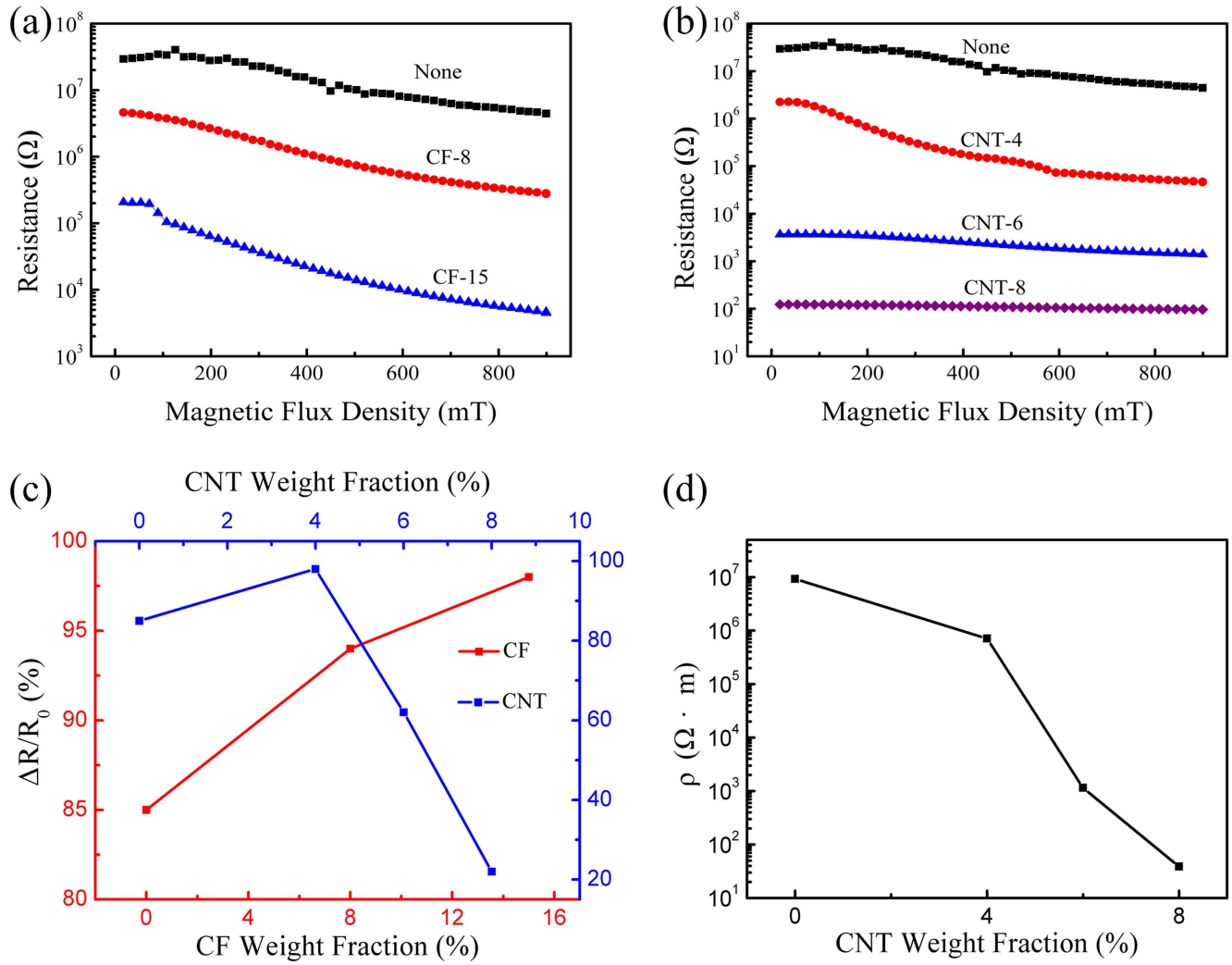

Figure 4. (a) and (b) were the resistance of CMRPs in different magnetic flux density: (a) CMRPs with different CF contents corresponding to 8 wt%, 15 wt%, (b) CMRPs with different CNT contents corresponding to 4 wt%, 6 wt%, 8 wt%. (c) The relative resistivity ($\Delta R/R_0$) of the CMRPs with different CF and CNT contents. ΔR was an increase of resistance with the magnetic flux density increasing from 0 to 900 mT. R_0 was the resistance under a 0 mT magnetic field. (d) The volume resistivity (ρ) of CMRPs with different CNT contents.

1.38 MPa, and the saturation G' decreased to 1.77 MPa, the relative MR effect was only 28%.

In this work, due to the low density, the CNTs formed a dense network structure within the matrix and thus hindered the movement of iron powders. Under application of the magnetic field, the increment of the storage modulus was small due to the weak magnetic dipole–dipole interaction between the far away CIPs. For CFs, they depicted a larger size than the CNTs, thus the as-formed networks were sparse. These micro-rods exhibited a smaller hinderance on iron powders than CNTs. Moreover, there would be many physical crosslinking points between the CFs and the CIPs chains formed under applying the magnetic field. These complex structures inevitably increased the storage modulus of the CMRPs, thus the enhanced MR effects were achieved. Based on the above results, it could be concluded that the CNTs affected the particle chains and too many CNTs presented a negative influence on the mechanical properties of CMRPs. As a comparison, the suitable ratio of CFs was favored for the MR effect.

Because of the conductive CFs and CNTs, the conductivity of the final CMRPs was improved. Figures 4(a), (b) showed the effect of CF and CNT contents on the resistance. Before the tests, a 900 mT magnetic field was first applied for 5 min to ensure the CIPs in the CMRPs be aggregated to form a chain structure. When the CFs and CNTs were introduced, the resistances decreased, respectively. The initial resistance (R_0) of 15 wt% CF-CMRPs was about two orders of magnitude lower than that of non-doped MRPs. Moreover, the R_0 of the 8 wt% CNT-CMRPs reduced by about five orders of magnitude lower than that of non-doped MRPs. Therefore, the CNTs were more effective for improving the conductivity than CFs because more electro-paths would be formed in the MRPs.

Interestingly, the resistance of the MRPs decreased with an increase in the magnetic field. Under a 900 mT magnetic field, the resistance of 8 wt% CF-CMRPs decreased to $2.76 \times 10^5\ \Omega$, and the resistance of 8 wt% CNT-CMRPs decreased to 97 Ω, which was reduced by four orders of magnitude than the equivalent weight CFs doped MRPs'

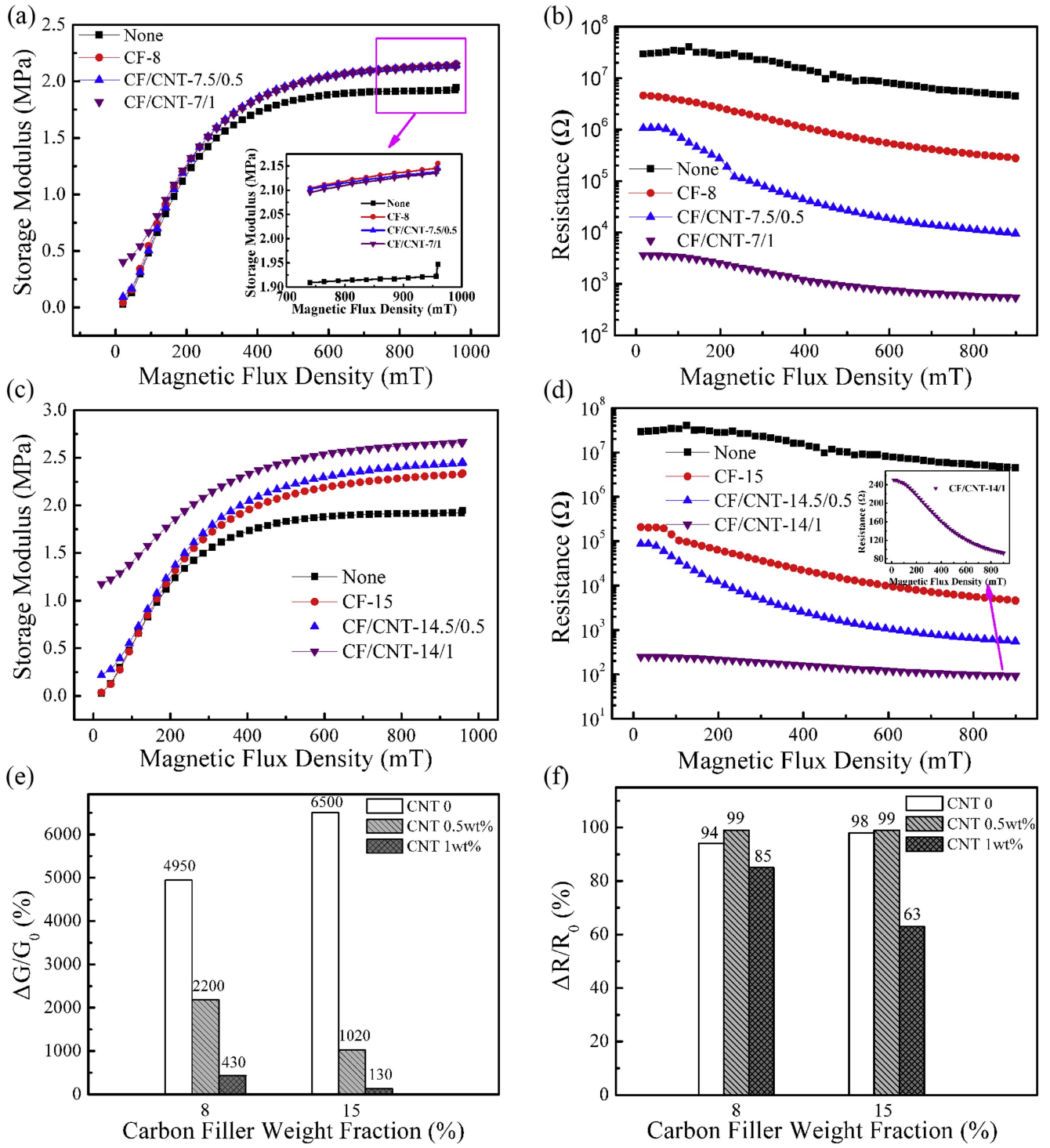

Figure 5. The storage modulus and resistance of CMRPs in different magnetic flux density. (a) and (b) CMRPs with 8 wt% CF contents, a mixture of 7.5 wt% CF and 0.5 wt% CNT, a mixture of 7 wt% CF and 1 wt% CNT. (c) and (d) CMRPs with 15% CF contents, a mixture of 14.5 wt% CF and 0.5 wt% CNT, a mixture of 14 wt% CF and 1 wt% CNT. (e) and (f) were the relative MR effect ($\Delta G'/G_0'$) and the relative resistivity ($\Delta R/R_0$) of CMRPs.

resistance. The relative resistivity ($\Delta R/R_0$) of 8 wt% CF-CMRPs was 94%, but the relative resistivity of 8 wt% CNT-CMRPs was only 22% (figure 4(c)). It further demonstrated that the CNTs had a good electrical conductivity, but hindered the movement of CIPs, which affected the formation of particle chains, thus the CNT-CMRPs had a lower MR effect. Here, the influence of the CNT concentration on the volume resistivity (ρ) was studied. From figure 4(d), it was observed that ρ decreased with an increase of the CNT content. The ρ values of the 4 wt% CNT-CMRPs and 8 wt% CNT-CMRPs were $7.05 \times 10^5\,\Omega$ and $3.87 \times 10^1\,\Omega$ respectively, which indicated the percolation threshold was between 4 and 8 wt%.

Based on the above result, it can be estimated that ideal multifunctional MRPs could be obtained by doping both of

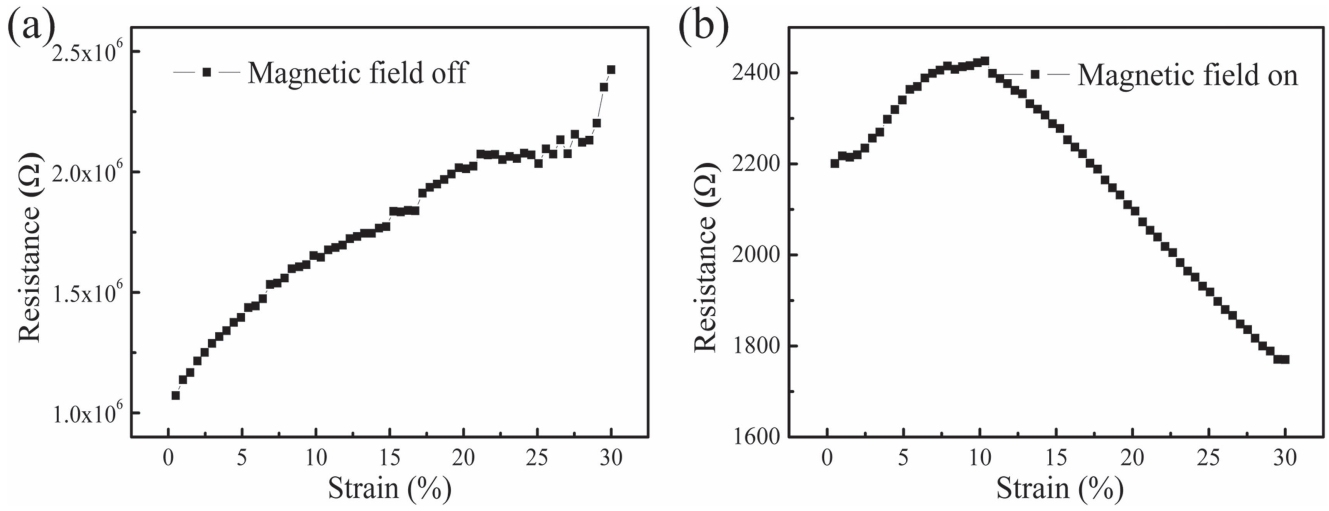

Figure 6. The resistance of CMRP filled with 7.5 wt% CFs and 0.5 wt% CNTs under the strain increasing from 0% to 30%. (a) Without magnetic field; (b) under a 900 mT magnetic field. The sample was 20 mm in diameter and 1 mm in thick. The strain increased linearly from 0% to 30%. The test time was 60 s.

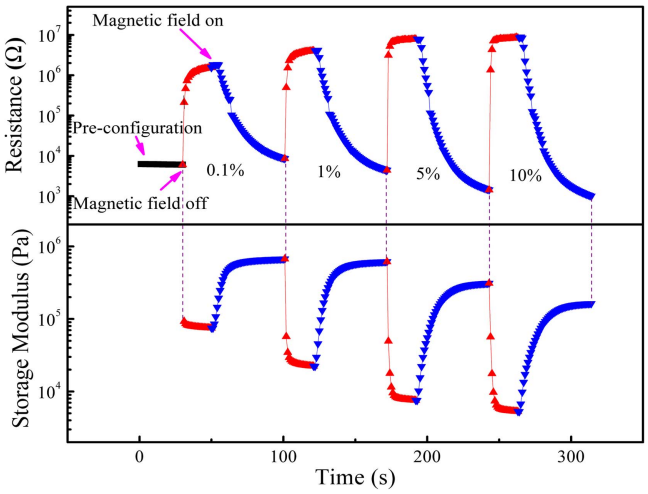

Figure 7. The resistance of CMRPs filled with 7.5 wt% CFs and 0.5 wt% CNTs. Such as: under a oscillation shear with a step amplitude which was 0.1%, 1%, 5%, 10%, respectively. The red dots showed the test results without the magnetic field, and the blue showed the test results with a magnetic field increasing from 0 to 900 mT.

the CFs and CNTs together within composite (CF/CNT-CMRPs). Therefore, there must be a optimum CFs/CNTs ratio for CF/CNT-CMRPs with both excellent mechanical and conductive properties. In this work, by keeping the total weight of the CFs/CNTs constant, the influence of the CNTs ratio in the CFs/CNTs hybrids was studied. As shown in figure 5, the saturation G' of CMRPs increased with carbon filler contents. The G' of CMRPs with 8 wt% carbon fillers under a 900 mT magnetic field was 0.2 MPa higher than that of the MRPs without carbon fillers (figure 5(a)). When the content of carbon fillers was 15%, the saturation G' increased by 0.72 MPa (figure 5(b)). Similarly, the relative MR effect decreased with the CNT contents. As shown in figure 5(e), the relative MR effect of CF/CNT (7/1)-CMRPs was 430%, which was 1/5 of the CF/CNT (7.5/0.5)-CMRPs' and 1/10 of non-doped MRPs'. Moreover, in case of 15 wt% carbon fillers doped MRPs, the relative MR effect of CF/CNT (14/1)-CMRPs was only 130%, which was 1/8 of CF/CNT (14.5/0.5)-CMRPs' and 1/50 of non-doped MRPs'.

Moreover, the resistance of CF/CNT-CMRPs decreased sharply with increasing CNT contents. In absence of the magnetic field, the R_0 of CF/CNT (7.5/0.5)-CMRPs was reduced by one order of magnitude less than that of non-doped MRPs and the R_0 of CF/CNT (7/1)-CMRPs was reduced by four orders of magnitude. When applying a magnetic field, the resistance of the CMRPs decreased in different degrees. The resistance of CF/CNT (14.5/0.5)-CMRPs decreased from 8.80×10^4 to $5.43 \times 10^2\ \Omega$ and the resistance of CF/CNT (14/1)-CMRPs decreased from 250 to 91 Ω with the magnetic field increasing from 0 to 900 mT. This result indicated that the CF/CNT-CMRPs showed excellent conductivity. Figure 5(f) showed the influence of magnetic field on CMRPs with different carbon filler contents. The relative resistivity ($\Delta R/R$) of CF/CNT (7.5/0.5)-CMRPs and CF/CNT (14.5/0.5)-CMRPs were 99%, which was higher than that of others (8 wt% CF-CMRPs, CF/CNT (7/1)-CMRPs, 15 wt% CF-CMRPs, CF/CNT (14/1)-CMRPs). That was to say, a certain number of CNTs can improve the relative resistivity, but CMRPs with too many or too few CNTs were not sensitive to the magnetic field. In summary, CF/CNT (7.5/0.5)-CMRPs had best mechanical and electrical properties. More importantly, the conductivity of the CF/CNT-CMRPs with a CF/CNT ratio of 7.5/0.5 was most easily controlled by magnetic field.

Besides the magnetic field, the influence of strain on the resistance of CMRPs was also investigated. Take the CF/CNT (7.5/0.5)-CMRPs as a example (figure 6). In the absence of the magnetic field, the resistance increased by 1.5 MΩ with the strain increasing from 0% to 30%. In contrast, the resistance first increased slightly and then decreased by 400 Ω under the 900 mT magnetic field. As we know, the particle chains in the CMRPs were destroyed due to the shear strain. Without the magnetic field, the conductive network

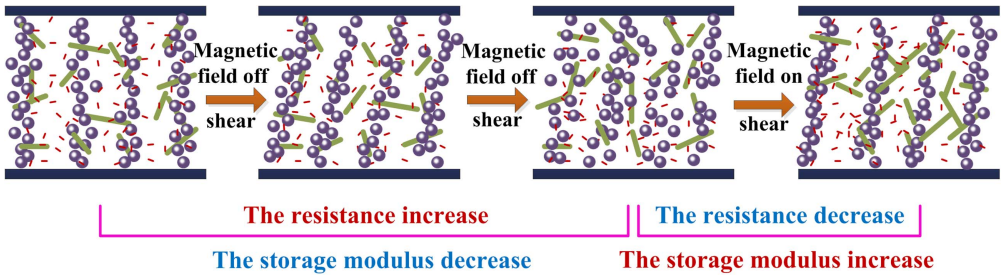

Figure 8. The microstructure evolution of CMRPs during the oscillatory shear. Purple balls represent the iron particles, green lines represent the carbon fibers, red lines represent the carbon nanotubes.

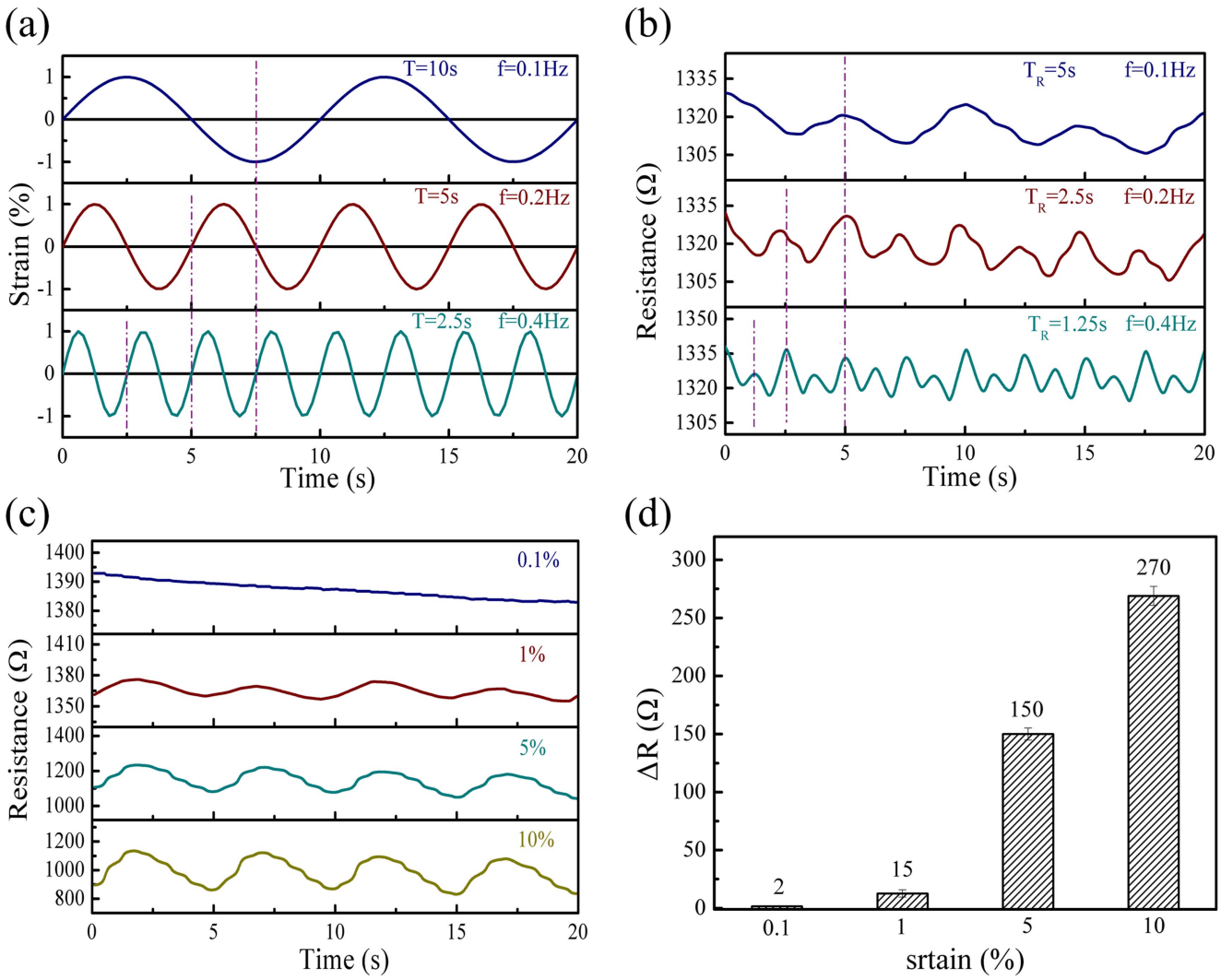

Figure 9. (a) The strain and (b) the resistance at different oscillation frequencies. The oscillation amplitude was 1% and the oscillation frequencies were 0.1 Hz, 0.2 Hz, 0.4 Hz, respectively. (c) The resistance and (d) the change in resistance at different oscillation amplitude. The oscillation frequency was 0.1 Hz and the oscillation amplitudes were 0.1%, 1%, 5%, 10%, respectively.

composed of CFs and CNTs would be destroyed thus the conductivity decreased. In the presence of a magnetic field, the increase of the resistance at the beginning was due to the abrupt application of shear strain leading to the destruction of the pre-structured particle chains. As the test time grew, the scattered iron powders would closely arrange along with the magnetic field and chains were reconstructed. In this case, the movement of the iron powders drove the CFs and the CNTs to connect with iron particle chains to form a better conductive network, thus the conductivity increased.

To further investigate the relationship between the resistance and the inner-structure of CMRPs, the resistance and the storage modulus of CMRPs under a different dynamic shear oscillation mode were tested. The shear amplitudes were 0.1%,

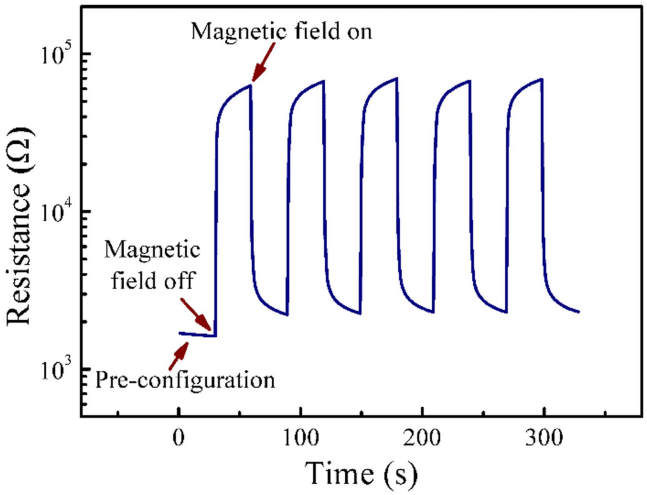

Figure 10 The resistance of the sample under magnetic fields alternately turned on and off. The magnetic flux density was 900 mT.

1%, 5%, 10%, respectively. Every shear oscillation process occurred with the alternation of magnetic field on and off. In figure 7, the resistance increased from 1.44×10^3 to $8.34 \times 10^6\,\Omega$ with 10% oscillation amplitude in the absence of magnetic field, and the storage modulus decreased from 5.65×10^4 to 5.31×10^3 Pa. When the magnetic field was applied, the resistance decreased from 8.34×10^6 to $1 \times 10^3\,\Omega$ and the storage modulus increased from 5.31×10^3 to 1.63×10^4 Pa. This further confirmed the particle chains were destroyed by strain and re-formed due to application of the magnetic field. It was found that the larger the amplitude of the oscillation, the greater the range of resistance variations.

Figure 8 illustrated the microstructure evolution of the resistance and storage modulus of CMRPs under a dynamic shear mode. When oscillatory shear occurred, the pre-configuration particle chains were tilted. With increasing amplitude of the oscillation, the iron powder particle chains were broken. That was why the resistance increased and the G' decreased. At this time, a magnetic field was applied, and the iron particles re-formed new chains with the surrounding particles and more closely with each other. So the resistance decreased sharply and the G' increased correspondingly. Due to the shear oscillation and the magnetic field, CFs and CNTs moved with the iron particles to form a better conductive network.

The influences of the frequencies on strain and resistance during one oscillation period were investigated. The experiments were carried out at a 900 mT magnetic field. As shown in figure 9(a), the oscillation amplitude was 1% and the oscillation frequencies were 0.1 Hz, 0.2 Hz, 0.4 Hz, respectively. The trend of strain with time was sinusoidal. The periods were 10 s, 5 s, 2.5 s, respectively. Interestingly, the trend of resistance with time was also sinusoidal (figure 9(b)). Moreover, the periods of resistance were 5 s, 2.5 s, 1.25 s, respectively. It was found that the resistance change period was half of the strain change period.

The resistance at different oscillation amplitudes which were 0.1%, 1%, 5%, 10% was shown in figure 9(c). The oscillation frequency was 0.1 Hz. Clearly, with an increasing oscillation amplitude, the change range of resistance also increased. As shown in figure 9(d), at 0.1% oscillation amplitude, the change in resistance was only 2 Ω. As soon as the oscillation amplitude was 10%, the range of resistance was 270 Ω. This showed that the resistance changed with the strain. The larger the strain variation range, the greater the resistance variation range.

Figure 10 showed the recovery and repeatability of the resistance of the CMRPs in the case where the magnetic field alternately turned on and off. The sample was placed in a 900 mT magnetic field for 15 min before testing. The magnetic field was then switched on and off alternately, each lasting for 30 s. It can be seen that when the magnetic field was turned on the resistance can be quickly reduced to $2 \times 10^3\,\Omega$. When the magnetic field was turned off, the resistance quickly rose to $6 \times 10^4\,\Omega$. Clearly, the peak of the resistance of each alternating process was almost the same. This showed that the recovery of the resistance was good and the sample can be reused.

4. Conclusions

In this study, a novel multifunctional MRPs strengthened with 1D CFs/CNTs carbon filler were developed. It can be found that CFs and CNTs improved the MR effects and conductivity of the MRP, respectively. Therefore, the combination of CFs and CNTs in MRPs was favorable for both the mechanical and electrical properties. When the CFs/CNTs ratio was 7.5/0.5 wt%, both the mechanical properties and conductivity of the CFs/CNTs-CMRPs were highly dependent on the magnetic field. G' increased by 2 MPa and the resistance was reduced by two orders of magnitude with the magnetic field increasing from 0 to 900 mT. Interestingly, the relative MR effect could reach 2200% for this concentration. More importantly, we can choose the appropriate ratio of CFs and CNTs according to the practical application. For instance, some applications required higher MR effects and the ratio of CFs should be higher and other applications needed higher conductivity and thus the ratio of CNTs should be higher. In addition, we applied an oscillatory shear with different amplitudes to the CMRPs. It can be concluded that the resistance increased by three orders of magnitude in the absence of a magnetic field and decreased by three orders of magnitude after applying a magnetic field. Furthermore, the period of the resistance was half of the strain and the amplitude of the resistance increased with the strain amplitude. Finally, the CFs/CNTs-CMRPs presented a excellent recyclable magnetic field dependent conductivity, which exhibited broad potential in their further applications.

Acknowledgments

Financial support from the National Natural Science Foundation of China (Grant No. 11572309, 11572310), the Strategic Priority Research Program of the Chinese

Academy of Sciences (Grant No. XDB22040502), and the Fundamental Research Funds for the Central Universities (WK2480000002) is gratefully acknowledged. This study was also supported by the Collaborative Innovation Center of Suzhou Nano Science and Technology.

References

[1] Sohn J W, Oh J S and Choi S B 2015 Design and novel type of a magnetorheological damper featuring piston bypass hole *Smart Mater. Struct.* **24** 035013
[2] Xing Z, Yu M, Sun S, Fu J and Li W 2015 A hybrid magnetorheological elastomer-fluid (MRE-F) isolation mount: development and experimental validation *Smart Mater. Struct.* **25** 015026
[3] Li W, Yao G, Chen G, Yeo S and Yap F 2000 Testing and steady state modeling of a linear MR damper under sinusoidal loading *Smart Mater. Struct.* **9** 95
[4] Raja P, Wang X and Gordaninejad F 2013 A high-force controllable MR fluid damper-liquid spring suspension system *Smart Mater. Struct.* **23** 015021
[5] Nguyen Q H and Choi S B 2009 Optimal design of MR shock absorber and application to vehicle suspension *Smart Mater. Struct.* **18** 2202–21
[6] Sun S, Yang J, Li W, Deng H, Du H, Alici G and Yan T 2016 An innovative MRE absorber with double natural frequencies for wide frequency bandwidth vibration absorption *Smart Mater. Struct.* **25** 055035
[7] Sun S, Yang J, Li W, Deng H, Du H and Alici G 2015 Development of an MRE adaptive tuned vibration absorber with self-sensing capability *Smart Mater. Struct.* **24** 095012
[8] Brigley M, Choi Y T, Wereley N M and Choi S-B 2007 Magnetorheological isolators using multiple fluid modes *J. Intell. Mater. Syst. Struct.* **18** 1143–8
[9] Przybylski M, Sun S and Li W 2016 Development and characterization of a multi-layer magnetorheological elastomer isolator based on a Halbach array *Smart Mater. Struct.* **25** 105015
[10] Yu M, Zhao L, Fu J and Zhu M 2016 Thermal effects on the laminated magnetorheological elastomer isolator *Smart Mater. Struct.* **25** 115039
[11] Behrooz M, Wang X and Gordaninejad F 2014 Modeling of a new semi-active/passive magnetorheological elastomer isolator *Smart Mater. Struct.* **23** 045013
[12] Yang J, Gong X, Zong L, Peng C and Xuan S 2013 Silicon carbide-strengthened magnetorheological elastomer: preparation and mechanical property *Polym. Eng. Sci.* **53** 2615–23
[13] Hato M J, Choi H J, Sim H H, Park B O and Ray S S 2011 Magnetic carbonyl iron suspension with organoclay additive and its magnetorheological properties *Colloids Surf.* A **377** 103–9
[14] Shah K, Seong M S, Upadhyay R and Choi S B 2013 A low sedimentation magnetorheological fluid based on plate-like iron particles, and verification using a damper test *Smart Mater. Struct.* **23** 027001
[15] Bekyarova E, Thostenson E, Yu A, Kim H, Gao J, Tang J, Hahn H, Chou T W, Itkis M and Haddon R 2007 Multiscale carbon nanotube-carbon fiber reinforcement for advanced epoxy composites *Langmuir* **23** 3970–4
[16] Stynoski P, Mondal P and Marsh C 2015 Effects of silica additives on fracture properties of carbon nanotube and carbon fiber reinforced Portland cement mortar *Cem. Concr. Compos.* **55** 232–40
[17] Chen L, Yin X, Fan X, Chen M, Ma X, Cheng L and Zhang L 2015 Mechanical and electromagnetic shielding properties of carbon fiber reinforced silicon carbide matrix composites *Carbon* **95** 10–9
[18] Bui H T, Tran B T, Le D Q, Than X T, Doan D P and Phan N M 2011 The effect of sintering temperature on the mechanical properties of a Cu/CNT nanocomposite prepared via a powder metallurgy method *Adv. Nat. Sci.: Nanosci. Nanotechnol.* **2** 015006
[19] Zylka P 2015 Biomimetic surface-conducting silicone rubber obtained by physical deposition of MWCNT *Smart Mater. Struct.* **24** 065040
[20] Gojny F, Wichmann M, Köpke U, Fiedler B and Schulte K 2004 Carbon nanotube-reinforced epoxy-composites: enhanced stiffness and fracture toughness at low nanotube content *Compos. Sci. Technol.* **64** 2363–71
[21] Kumar A, Maschmann M R, Hodson S L, Baur J and Fisher T S 2015 Carbon nanotube arrays decorated with multi-layer graphene-nanopetals enhance mechanical strength and durability *Carbon* **84** 236–45
[22] Baechler C, Gardin S, Abuhimd H and Kovacs G 2016 Inkjet printed multiwall carbon nanotube electrodes for dielectric elastomer actuators *Smart Mater. Struct.* **25** 055009
[23] Mo L, Ran J, Yang L, Fang Y, Zhai Q and Li L 2016 Flexible transparent conductive films combining flexographic printed silver grids with CNT coating *Nanotechnology* **27** 065202
[24] Abot J L, Kiyono C Y, Thomas G P and Silva E C 2015 Strain gauge sensors comprised of carbon nanotube yarn: parametric numerical analysis of their piezoresistive response *Smart Mater. Struct.* **24** 075018
[25] Li A, Bogdanovich A E and Bradford P D 2015 Aligned carbon nanotube sheet piezoresistive strain sensors *Smart Mater. Struct.* **24** 095004
[26] Zang X, Xu R, Zhang Y, Li X, Zhang L, Wei J, Wang K and Zhu H 2015 All carbon coaxial supercapacitors based on hollow carbon nanotube sleeve structure *Nanotechnology* **26** 045401
[27] Rangom Y, Tang X and Nazar L F 2015 Carbon nanotube-based supercapacitors with excellent ac line filtering and rate capability via improved interfacial impedance *ACS Nano* **9** 7248–55
[28] Qin W, Vautard F, Drzal L T and Yu J 2015 Mechanical and electrical properties of carbon fiber composites with incorporation of graphene nanoplatelets at the fiber–matrix interphase *Composites* B **69** 335–41
[29] Drubetski M, Siegmann A and Narkis M 2007 Electrical properties of hybrid carbon black/carbon fiber polypropylene composites *J. Mater. Sci.* **42** 1–8
[30] An X, Ma J, Wang K and Zhan M 2016 Growth of silver nanowires on carbon fiber to produce hybrid/waterborne polyurethane composites with improved electrical properties *J. Appl. Polym. Sci.* **133** 43056
[31] Pal G and Kumar S 2016 Multiscale modeling of effective electrical conductivity of short carbon fiber-carbon nanotube-polymer matrix hybrid composites *Mater. Des.* **89** 129–36
[32] Zhang F-H, Wang R G, He X D, Wang C and Ren L-N 2009 Interfacial shearing strength and reinforcing mechanisms of an epoxy composite reinforced using a carbon nanotube/carbon fiber hybrid *J. Mater. Sci.* **44** 3574–7
[33] Li R and Sun L 2011 Dynamic mechanical behavior of magnetorheological nanocomposites filled with carbon nanotubes *Appl. Phys. Lett.* **99** 131912
[34] Ko S, Lim J, Park B, Yang M and Choi H 2009 Magnetorheological carbonyl iron particles doubly wrapped with polymer and carbon nanotube *J. Appl. Phys.* **105** 07E703
[35] Reddy S K, Mukherjee A and Misra A 2014 Magnetic field induced tailoring of mechanical behavior of fluid filled micro porous carbon nanotube foam *Appl. Phys. Lett.* **104** 261906

[36] Jang S and Yin H 2015 Effect of aligned ferromagnetic particles on strain sensitivity of multi-walled carbon nanotube/polydimethylsiloxane sensors *Appl. Phys. Lett.* **106** 141903

[37] Yang P, Yu M and Fu J 2016 Ni-coated multi-walled carbon nanotubes enhanced the magnetorheological performance of magnetorheological gel *J. Nanopart. Res.* **18** 1–11

[38] Pang H, Xuan S, Liu T and Gong X 2015 Magnetic field dependent electro-conductivity of the graphite doped magnetorheological plastomers *Soft Matter* **11** 6893–902

[39] Wang S, Xuan S, Jiang W, Jiang W, Yan L, Mao Y, Liu M and Gong X 2015 Rate-dependent and self-healing conductive shear stiffening nanocomposite: a novel safe-guarding material with force sensitivity *J. Mater. Chem.* A **3** 19790–9